XVI International Conference on Computational Plasticity. Fundamentals and Applications
COMPLAS 2021
E. Oñate, D. Peric, M. Chiumenti and Eduardo de Souza Neto (Eds)

EVALUATION OF FOUR ADVANCED PLASTICITY AND HYPOPLASTICITY MODELS IN SIMULATING CYCLIC RESPONSE OF SANDS

Jose Duque[1*], Ming Yang[2], William Fuentes[3], David Mašín[1] and Mahdi Taiebat[2]

[1*] Institute of Hydrogeology, Engineering Geology and Applied Geophysics. Charles University, Prague, Czech Republic. email: duquefej@natur.cuni.cz

[2] Department of Civil Engineering. University of British Columbia, Vancouver, Canada

[3] Findeter. Bogotá, Colombia

Key words: Cyclic loading, elastoplasticity, hypoplasticity, limitations

Abstract. Numerous constitutive models have been developed for the simulation of the response of granular soils under cyclic loading. While these models have succeeded in capturing certain aspects of the stress-strain response under a number of idealized loading paths, certain common limitations are encountered in simulating these and other paths, and also certain complex aspects of response. Examples of these include cyclic oedometeric stiffness, shear strain accumulation in cyclic mobility, cyclic liquefaction strength curves, among others. These limitations are rather crucial for the end-users. Discussing these limitations and providing the mechanisms to avoid them if possible, therefore, would be of great value for both applications and further developments. Relying on cyclic loading experimental test data of Karlsruhe fine sand, the present study conducts direct comparison between the experiments and the corresponding simulation results using four advanced constitutive models: two bounding surface elastoplasticity [1, 2] and two hypoplasticity models [3, 4] – with the models in each category following a hierarchical order of complexity. The presented results elaborate on the specific capabilities and limitations of these advanced models in simulating several essential aspects of cyclic loading of sands.

1 Introduction

Continuous development and improvement of constitutive models in simulating the cyclic response of soils have been carried out by a number of researchers in recent decades, e.g., [1, 2, 3, 4, 5, 6, 7, 8, 9, 10, 11, 12], just to mention a few. Some of these models have properly taken into account void ratio and stress dependency on the strength and stiffness characteristics and incorporated small strain stiffness effects to capture relevant aspects in cyclic loading. Despite these achievements, detailed evaluation of their performance in simulation of certain cyclic paths of more complex nature reveals some important deficiencies which are shared by many models. These deficiencies deserve to be discussed and carefully analyzed in order to explore their causes and to propose solutions to avoid them. Examples of them include overshooting after reverse loading/immediate reloading paths, shear strain accumulation in cyclic mobility, inadequate simulation of cyclic liquefaction strength curves, inability to reach stress attractors of dense samples under cyclic undrained loading, improper accumulation of strains and/or pore water pressure in cyclic shearing with small amplitudes, inaccurate cyclic oedometric stiffness, missing memory effect of drained preloading in subsequent undrained shearing, among others.

Some of these shortcomings have been properly resolved via introducing new mechanisms on existing models while others still deserve extra attention. Thus it is worthwhile to identify the common limitations of the advanced constitutive models for cyclic loading and carefully investigate their causes with the goal to come up with the corresponding mechanisms and formulations to avoid them if possible.

This paper focuses on presenting and analyzing three limitations out of many which have been observed in simulations of cyclic loading paths, including adequate modeling of cyclic oedometric stiffness, shear strain accumulation in cyclic mobility, and cyclic liquefaction strength curves. While the present paper briefly discusses only these three limitations, a more comprehensive version of this study can be found in Duque et al. [13]. In the analysis, four advanced constitutive models are selected: the bounding surface plasticity model accounting for fabric changes on dilatancy proposed by Dafalias and Manzari [1], hereafter denoted as DM04, the recently proposed model incorporating memory surface and semifluidized state into DM04 by Yang et al. [2], denoted as SANISAND-MSf, the hypoplastic model for sands with Intergranular Strain (IS) by Niemunis and Herle [3], henceforth denoted as HP+IS model, and the hypoplastic model for sands extended with Intergranular Strain Anisotropy (ISA) by Fuentes et al. [4], denoted as HP+ISA model. An exercise of self-criticism and discussion of why these models are able or unable to reproduce properly the expected response is conducted according to the authors' experience with the selected models.

2 Analysis of some relevant limitations in the simulation of cyclic loading

While the readers are referred to the relevant publications for the details of the selected constitutive models, here we directly present the comparisons between experiments and simulation results. We choose the laboratory element tests of Karlsruhe fine sand [14, 15] as the experimental database. The four selected constitutive models are calibrated against Karlsruhe fine sand, with the model constants presented in Tables 1 and 2, respectively.

2.1 Cyclic oedometric stiffness

Oedometric tests are of particular importance for settlement predictions on many engineering problems. When the vertical loading is of cyclic nature, and occurs under drained conditions, correct assessment of cyclic models on the reproduction of oedometric cycles is of crucial relevance. Although a cyclic oedometer test is considered to be simple, yet important, many deficiencies have been seen on their simulations. Problems concerning to the resulting oedometric stiffness, and overshooting/subshooting effects are characteristic drawbacks on these simulations. For illustration and analysis purposes, a cyclic

Table 1: Model constants of DM04 and SANISAND-MSf for Karlsruhe fine sand

Model constant	Nomenclature	DM04	SANISAND-MSf	Units
Elasticity	G_0	150	150	[-]
	ν	0.05	0.05	[-]
Critical state	M_c	1.34	1.34	[-]
	c	0.7	0.7	[-]
	λ_c	0.122	0.122	[-]
	$e_\mathrm{c}^\mathrm{ref}$	1.103	1.103	[-]
	ξ	0.205	0.205	[-]
Yield surface	m	0.05	0.05	[-]
Plastic modulus	h_0	10.5	10.5	[-]
	c_h	0.95	0.95	[-]
	n^b	1.2	1.2	[-]
Dilatancy	A_0	0.9	0.9	[-]
	n^d	2	2	[-]
	n_g	-	0.92	[-]
Fabric dilatancy	z_max	15	15	[-]
	c_z	2000	2000	[-]
Memory surface	μ_0	-	2.5	[-]
	u	-	1.2	[-]
Semifluidized state	x	-	5.5	[-]
	c_ℓ	-	30	[-]

oedometer test reported by Wichtmann and Triantafyllidis [15] on Karlsruhe fine sand is shown in Figure 1a and simulated with the selected constitutive models in Figures 1b-d, respectively. The oedometric test presents an initial void ratio of $e_0 = 0.8894$ and initial axial stress of $\sigma_1 = 0.221$ kPa. It consists of multiple unloading-reloading cycles with the loading/reloading paths increase the axial stress to a) $\sigma_1 = 20.53$ kPa, b) $\sigma_1 = 55.72$ kPa, c) $\sigma_1 = 142.14$ kPa, d) $\sigma_1 = 407.1$ kPa and e) $\sigma_1 = 407.1$ kPa, respectively. All unloading paths reach always $\sigma_1 = 1$ kPa.

From the simulations in Figure 1, one can draw the following conclusions: first, the DM04 and SANISAND-MSf models present in general a stiffer behavior. This is one of the consequences of using a narrow wedge-type open yield surface, which induces zero plasticity under constant stress-ratio loading. As a solution, Taiebat and Dafalias [16] proposed a mechanism for plastic strains under constant stress-ratio loading. On the other hand, the hypoplastic models extended by intergranular strain including HP+IS and HP+ISA perform better in capturing cyclic stiffness as they consider the void ratio characteristic loading curves, corresponding to the maximum, minimum and critical state void ratios in their formulations although they present something improper in the reloading paths, i.e., surpassing the envelope formed by the monotonic curve. The reason for why still overshootings/subshootings being observed in the simulations is simple.

Table 2: Model constants of HP+IS and HP+ISA for Karlsruhe fine sand

Model constant	Nomenclature	HP+IS	HP+ISA	Units
Critical state friction angle	φ_c	33.1	33.1	[°]
Granular hardness	h_s	4000	4000	[MPa]
Barotropy exponent	n	0.27	0.27	[-]
Dilatancy exponent	α	0.14	0.14	[-]
Pyknotropy exponent	β	2.5	2.5	[-]
Minimum void ratio at $p = 0$	e_{d0}	0.677	0.677	[-]
Critical void ratio at $p = 0$	e_{c0}	1.054	1.054	[-]
Maximum void ratio at $p = 0$	e_{i0}	1.212	1.212	[-]
Elastic strain amplitude	R	1×10^{-4}	1×10^{-4}	[-]
Stiffness factor for reversal loading	m_R	2.2	5	[-]
Stiffness factor for transversal loading	m_T	1.1	-	[-]
IS hardening parameter	β_r	0.1	-	[-]
Minimum IS hardening parameter	β_{h0}	-	0.2	[-]
Maximum IS hardening parameter	β_{hmax}	-	3	[-]
IS exponent	χ	5.5	-	[-]
Minimum IS exponent	χ_0	-	5	[-]
Maximum IS exponent	χ_{max}	-	17.7	[-]
Accumulation rate factor	c_a	-	0.018	[-]
Cyclic mobility factor	c_z	-	300	[-]

For both HP+IS and HP+ISA, upon loading reversal, the initial increased stiffness is gradually degraded along the reloading path. accorsing to the model, the amount of deformation required to degrade the stiffness is constant, and independent of the size (in terms of strain amplitude) of the previously performed unloading path. Incorporating an enhanced intergranular strain theory with an elastic locus, the HP+ISA model embraces a memory effect for cycles of very small strain amplitudes, whereby $\| \Delta\boldsymbol{\varepsilon} \| < R$, and R is a predefined material parameter $R \approx 10^{-4}$. This feature enables the good performance in the simulation of the first two cycles but needs extra revision to attain success in the subsequent cycles having larger strain amplitudes.

2.2 Shear strain accumulation in cyclic mobility

When medium dense or dense sand elements are subjected to undrained cyclic shearing with a constant shear stress amplitude, they experience a gradual reduction of mean effective stress p. For medium dense to dense samples, the material eventually undergoes the so-called cyclic mobility states, in which the stress path experiences typical butterfly shape with momentary liquefaction state (p near zero) while the cyclic strain amplitude increases cycle-by-cycle. Large but limited cyclic shear strain develops after a sufficient number of loading cycles. The simple shear experiments usually manifest rather symmet-

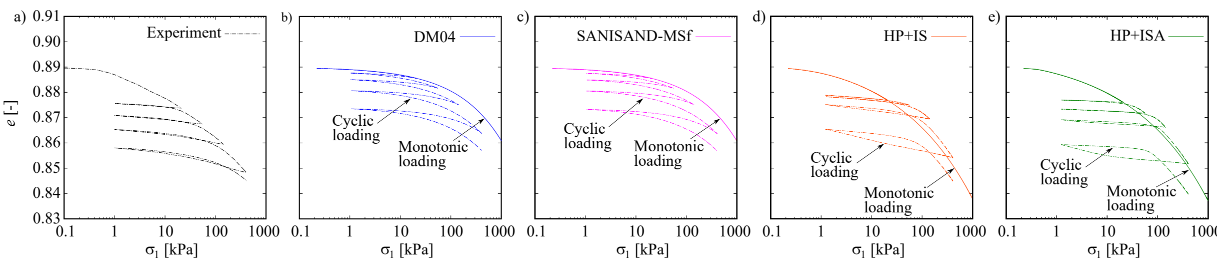

Figure 1: Cyclic oedometric test with multiple unloading-reloading cycles: a) Experiment on Karlsruhe fine sand; b) DM04; c) SANISAND-MSf; d) HP+IS; e) HP+ISA

ric stress-strain loops while the triaxial ones tend to accumulate more strain in the extension side compared with the compression side but still with stress-strain loops expanding on both sides. Figures 2a and b presents an undrained cyclic triaxial test of $q^{\mathrm{amp}} = 60$ kPa on Karlsruhe fine sand with initial mean stress $p_0 = 200$ kPa and $D_{\mathrm{r}} = 67\%$ [14]. Evidently, one can see the butterfly shape in Figure 2a and the increasing magnitudes of the maximum and minimum axial strains in each cycle along with the cycles in Figure 2b.

To numerically model this experiment, there should be two main considerations. The first is the large shear strain development in the liquefaction state with increasing amplitudes in subsequent cycles, and the second is the non-symmetric evolution of stress-strain loops, avoiding the whole shift of stress-strain loops to the extension side, i.e., one-way ratcheting. While some models have tackled the first difficulty e.g. [8, 9, 10, 17, 18], less success has been achieved on the second one, except a recent attempt [2].

Simulation results of the undrained cyclic triaxial test using DM04, SANISAND-MSf, HP+IS, and HP+ISA are presented in Figure 2c-j. Clearly all the models except HP+IS can achieve a satisfying butterfly shape in the stress path due to incorporation of the fabric-dilatancy tensor initially proposed by Dafalias and Manzari [1]. However, the simulated stress-strain loops of DM04, HP+IS and HP+ISA manifest the unrealistic one-way ratcheting. There are two reasons underlying this behavior. The first is that these critical state compatible models account for Lode's angle dependence in the critical state surface, inducing a much higher unbalance of the plastic strain rate in the compression and extension sides. With this properly resolved, these models still required a constitutive ingredient that allows for large shear strain development in the liquefaction state. The SANISAND-MSf is the only model able to reproduce the double amplitude of cyclic shear strains as it tackles the two aforementioned issues by introducing two additional constitutive ingredients in the model. The first is significantly reducing the dilatancy and plastic modulus at low mean effective stress or so-called semifluidized state, via a novel internal variable called "strain liquefaction factor" (SLF), which also evolves only at low effective stresses. This mechanism, originally proposed by Barrero et al. [8], is to reproduce shear strain development in the liquefaction state. The second consists of influencing the dilatancy and plastic modulus by a Lode angle dependent term controlled by model parameter n_g as listed in Table 2, with the goal to balance the relative magnitude of shear strain amplitudes in triaxial compression and extension.

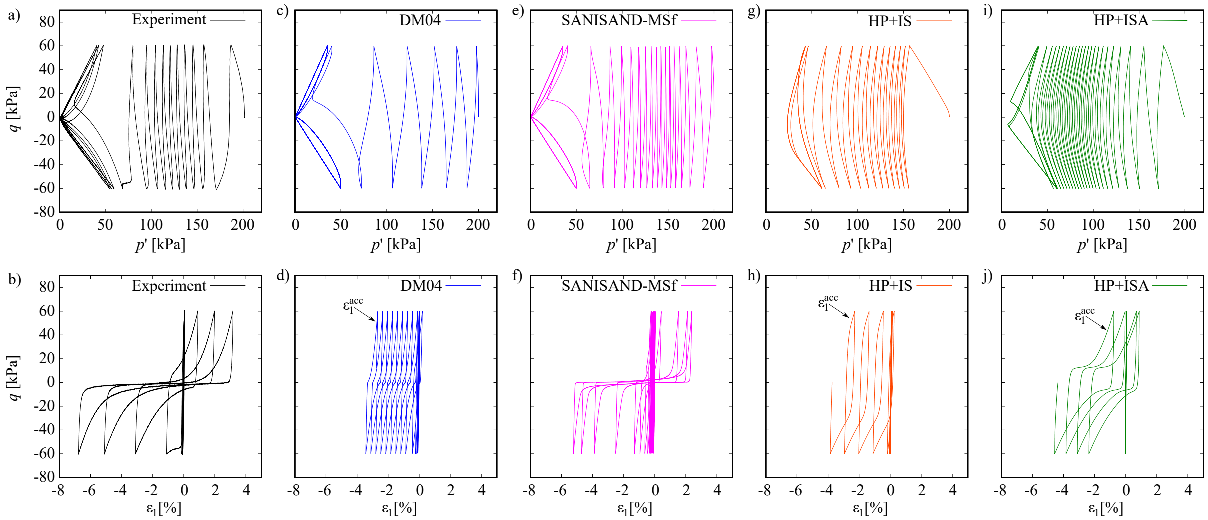

Figure 2: Undrained cyclic triaxial test on Karlsruhe fine sand. Medium density sample (D_{r} = 67%) with isotropic consolidation (p_0 = 200 kPa) and stress cycles of q^{amp} = 60 kPa: a,b) Experiment c,d) DM04; e,f) SANISAND-MSf; g,h) HP+IS; i,j)HP+ISA

2.3 Cyclic liquefaction strength curves

Cyclic liquefaction failure is usually defined as the state at which excess pore pressure ratio approaches 1, or at which the single or double strain amplitudes reach some limiting values. Cyclic liquefaction of saturated sand can be triggered by different combinations of uniform cyclic stress ratio (CSR), which is the uniform cyclic shear stress divided by initial effective confining stress, and the number of loading cycles [19]. The liquefaction strength curve, i.e., the plot of CSR versus the number of cycles to initial liquefaction N_{ini}, are of practical importance for assessing the success of a sand constitutive model in simulation of cyclic liquefaction.

Under cyclic triaxial conditions, the CSR is defined as the ratio of the deviatoric stress to two times the initial mean effective stress, i.e. CSR $= q^{\mathrm{amp}}/(2p_0)$. In this paper, the following criteria for initial liquefaction are considered: a) excess pore water pressure ratio $r_u = 0.95$, b) axial strain in single amplitude of $\varepsilon_1^{\mathrm{SA}} = 2.5\%$, and c) axial strain in double amplitude of $\varepsilon_1^{\mathrm{DA}} = 5\%$. The performance of the selected constitutive models is evaluated based on the liquefaction strength curves of Karlsruhe fine sand. For the construction of the CSR–N_{ini} curves, a database of undrained cyclic triaxial tests reported by Wichtmann and Triantafyllidis [14] is employed. The analysis is performed on samples with medium density, with a mean relative density of 63% and an initial mean effective stress $p_0 = 100$ kPa, covering a range of CSRs. The CSR–N_{ini} curves of Karlsruhe fine sand for the three liquefaction criteria are presented in Figure 3.

Simulations with the DM04 model show much steeper strength curves than the experiments for the criteria of $r_u = 0.95$ and $\varepsilon_1^{\mathrm{SA}} = 2.5\%$ as shown in Figure 3a,b. In addition, the DM04 simulations do not reach $\varepsilon_1^{\mathrm{DA}} = 5\%$ and so they are absent from Figure 3c. Recalling the stress-strain plots from the previous section, contrary to the experiments the DM04 shows a one-way ratcheting of strains in the extension direction,

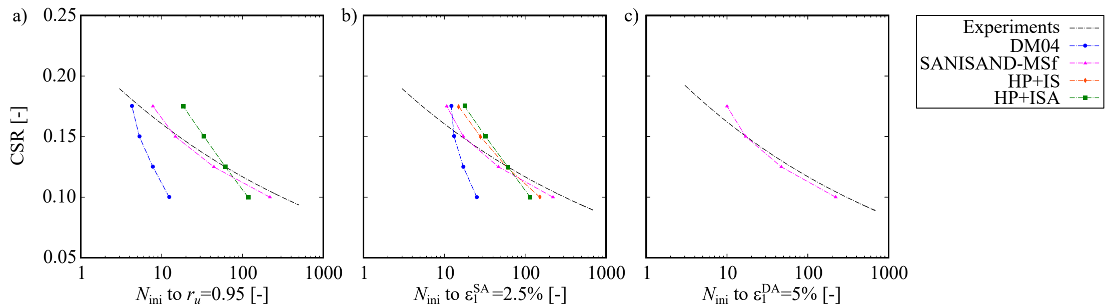

Figure 3: Liquefaction strength curves of Karlsruhe fine sand with medium dense samples and different liquefaction criteria

and that is why it reaches $\varepsilon_1^{\mathrm{SA}} = 2.5\%$ (yet not at correct number of cycles) but does not reach $\varepsilon_1^{\mathrm{DA}} = 5\%$. On the other hand, simulations with the SANISAND-MSf model show a significantly improved performance for all three liquefaction criteria. The number of cycles to reach the liquefaction criteria are improved due to the rule of the memory surface mechanism in the pre-liquefaction stage. The simulations of SANISAND-MSf also reach $\varepsilon_1^{\mathrm{DA}} = 5\%$ contrary to what was observed in case of DM04, with an accurate performance as shown in Figure 3b. This is due to the rule of the semifluidized state mechanism in the post-liquefaction stage.

The performance of the HP+IS model is not pleasant as it cannot reach the liquefaction criteria $r_u = 0.95$ or $\varepsilon_1^{\mathrm{DA}} = 5\%$, due to the lack of a cyclic mobility mechanism. The simulations can reach the $\varepsilon_1^{\mathrm{SA}} = 2.5\%$ criterion, but show steeper curves than the experiments. It should be remarked that this model also shows a one-way ratcheting of cyclic shear strain as shown in the previous section and that is why it reaches $\varepsilon_1^{\mathrm{SA}} = 2.5\%$ but not $\varepsilon_1^{\mathrm{DA}} = 5\%$. Finally, simulations with the HP+ISA model show that in contrast to the HP+IS, it is able to reach $r_u = 0.95$ due to the incorporation of cyclic mobility effects and a proper reproduction of the pore water pressure accumulation, but the simulated curves are steeper than the experimental ones. The liquefaction criterion $\varepsilon_1^{\mathrm{DA}} = 5\%$ was not reached with the model. The performance related to the criterion $\varepsilon_1^{\mathrm{SA}} = 2.5\%$ is very similar to that of the HP+IS model. Note that this model also shows a one-way accumulation of cyclic shear strains in the extension direction, as shown in the previous section.

3 Conclusions

This paper presents and discusses three common aspects of simulating cyclic response of sands using four advanced constitutive models, including cyclic oedometric stiffness, shear strain accumulation in cyclic mobility, and cyclic liquefaction strength curves. The four models consist of two from the bounding surface plasticity family and two from the hypoplastic family. For a more thorough study of this topic, readers are referred to Duque et al. [13]. The main conclusions are summarized as follows:

- The bounding surface elastoplasticity models when formulated in terms of stress-ratio changes for generating plasticity, may deliver inadequate oedometric loading stiffness. For the case of hypoplasticity models, the incorporation of an active non-linear component allows for proper reproduction of plastic strains under this path.

- Simulation of cyclic mobility in undrained cyclic triaxial tests with symmetric deviator stress amplitude ($q^{\min} = q^{\max}$) is often accompanied with one-way ratcheting in strain accumulation. In the SANISAND-MSf model, two specific considerations significantly improved the simulation capability in modeling of cyclic mobility: introducing a simple Lode angle dependency and the concept of semifluidized state.

- The adequate modeling of cyclic liquefaction strength curves or CSR–N_{ini} considering various criteria for reaching initial liquefaction, is a challenge in majority of available constitutive models. Among the four models assessed in this study, only SANISAND-MSf shows capabilities in adequately capturing the cyclic liquefaction curve based on various liquefaction criteria including excess pore pressure ratio, and both single and double amplitudes of shear strain. The memory surface feature of the model allows for capturing the correct N_{ini} at various CSR level for reaching the r_u criterion, and the semifluidized state feature allows for capturing the criteria related to single and double amplitudes of shear strain.

4 Acknowledgements

The first and fourth authors appreciate the financial support given by the INTER-EXCELLENCE project LTACH19028 by the Czech Ministry of Education, Youth and Sports. The first author appreciates the financial support given by the Charles University Grant Agency (GAUK) with project number 200120. The first and fourth authors acknowledge institutional support by Center for Geosphere Dynamics (UNCE/SCI/006). The second and fifth authors acknowledge the support from the Natural Sciences and Engineering Research Council of Canada (NSERC).

REFERENCES

[1] Dafalias, Y. and Manzari, M. Simple plasticity sand model accounting for fabric change effects. *Journal of Engineering Mechanics* (2004) **130**(6):622–634.

[2] Yang, M., Taiebat, M. and Dafalias, Y. SANISAND-MSf: a sand plasticity model with memory surface and semifluidised state. *Géotechnique* (2021), doi: 10.1680/jgeot.19.P.363.

[3] Niemunis, A. and Herle, I. Hypoplastic model for cohesionless soils with elastic strain range. *Mechanic of cohesive-frictional materials* (1997) **2**(4):279–299.

[4] Fuentes, W., Wichtmann, T., Gil, M. and Lascarro, C. ISA-Hypoplasticity accounting for cyclic mobility effects for liquefaction analysis. *Acta Geotechnica* (2020) **15**:1513–1531.

[5] Dafalias, Y. and Taiebat, M. SANISAND-Z: zero elastic range sand plasticity model. *Géotechnique* (2016) **66**(12):999–1013.

[6] Prevost, J. A simple plasticity theory for frictional cohesionless soils. *Soil Dynamics and Earthquake Engineering* (1985) **4**(1):9–17.

[7] Elgamal, A., Yang, Z. and Parra, E. Computational modeling of cyclic mobility and post-liquefaction site response. *Soil Dynamics and Earthquake Engineering* (2002) **22**(4):259–271.

[8] Barrero, A., Taiebat, M. and Dafalias, Y. Modeling cyclic shearing of sands in the semifluidized state. *International Journal for Numerical and Analytical Methods in Geomechanics* (2020) **44**(3):371–388.

[9] Zhang, J. and Wang, G. Large post-liquefaction deformation of sand, part I: physical mechanism, constitutive description and numerical algorithm. *Acta Geotechnica* (2012) **7**(2):69–113.

[10] Boulanger, R. and Ziotopoulou, K. Formulation of a sand plasticity plane-strain model for earthquake engineering applications. *Soil Dynamics and Earthquake Engineering* (2013) **53**:254–267.

[11] Wang, Z.-L., Dafalias Y. F. and Shen, C.-K. Bounding surface hypoplasticity model for sand. *Journal of Engineering Mechanics* (1990) **116**(5): 983–1001.

[12] Fuentes, W., Triantafyllidis, T. and Lascarro, C. Evaluating the Performance of an ISA-Hypoplasticity Constitutive Model on Problems with Repetitive Loading. *Holistic Simulation of Geotechnical Installation Processes* (2017):341–362.

[13] Duque, J., Fuentes, W., Ming, Y., Mašín, D. and Taiebat, M. Characteristic limitations of advanced plasticity and hypoplasticity models for cyclic loading of sands *Under Review* (2021).

[14] Wichtmann, T. Soil behaviour under cyclic loading: Experimental observations, constitutive description and applications. *Habilitation, Karlsruhe Institute of Technology* (2016)

[15] Wichtmann, T. and Triantafyllidis, T. An experimental data base for the development, calibration and verification of constitutive models for sand with focus to cyclic loading. part I: tests with monotonic loading and stress cycles. *Acta Geotechnica* (2016) **11**(4):739–761.

[16] Taiebat, M. and Dafalias, Y. SANISAND, simple anisotropic sand plasticity model. *International Journal for Numerical and Analytical Methods in Geomechanics* (2008) **32**(8):915–948.

[17] Elgamal, A., Yang, Z., Parra, E. and Ragheb, A. Modeling of cyclic mobility in saturated cohesionless soils. *International Journal of Plasticity* (2003) **19**(6):883–905.

[18] Iai, S., Tobita, T., Ozutsumi, O. and Ueda, K.Dilatancy of granular materials in a strain space multiple mechanism model. *International Journal for Numerical and Analytical Methods in Geomechanics* (2011) **35**(3):360–392.

[19] Idriss, I. and Boulanger, R. Soil liquefaction during earthquakes. *Earthquake Engineering Research Institute* (2008).